communications biology

Article

https://doi.org/10.1038/s42003-024-06628-1

Combining *Bifidobacterium longum* subsp. *infantis* and human milk oligosaccharides synergistically increases short chain fatty acid production ex vivo

Check for updates

Florac De Bruyn [1] ✉, Kieran James[1], Geoffrey Cottenet[2], Maes Dominick[1] & Johnson Katja[1]

To enhance health benefits, a probiotic can be co-administered with a metabolizable prebiotic forming a synergistic synbiotic. We assessed the synergies resulting from combining *Bifidobacterium longum* subsp. *infantis* LMG 11588 and an age-adapted blend of six human milk oligosaccharides (HMOs) in ex vivo colonic incubation bioreactors seeded with fecal background microbiota from infant and toddler donors. When HMOs were combined with *B. infantis* LMG 11588, they were rapidly and completely consumed. This resulted in increased short chain fatty acid (SCFA) production compared to the summed SCFA production from individual ingredients (synergy). Remarkably, HMOs were partially consumed for specific infant donors in the absence of *B. infantis* LMG 11588, yet all donors showed increased SCFA production upon *B. infantis* LMG 11588 supplementation. We found specific bacterial taxa associated with the differential response pattern to HMOs. Our study shows the importance of carefully selecting pre- and probiotic into a synergistic synbiotic that could benefit infants.

The infant gut microbiota is enriched for *Bifidobacterium* species, particularly in full-term, healthy, breastfed infants. *Bifidobacterium longum* subsp. *infantis* is predominantly associated with the breastfed infant gut niche[1–6]. This *Bifidobacterium* subspecies has been associated with immune system maturation and enhanced gut barrier function, possibly even reducing the risk of gastrointestinal disorders such as necrotizing enterocolitis by modulating the gut microbiome and reducing inflammation[7,8]. One proposed mechanism of action for *B. infantis*-related health benefits acts through its efficient production of short-chain fatty acids (SCFAs), which can improve intestinal health and function[9]. This phenomenon is primarily thought to be due to its ability to prolifically consume a large diversity of human milk oligosaccharides (HMOs)[7,9]. HMOs are complex carbohydrates found in human milk that cannot be digested by human enzymes and are thus selective substrates for the growth of beneficial gut bacteria, including *B. infantis*[6]. The composition of the HMO fraction in human milk is both individual and postpartum-dependent[10–12]. *Bifidobacterium infantis* expresses a large arsenal of glycosyl hydrolases and carbohydrate transport systems, which enable it to efficiently import and intracellularly degrade HMO glycans with a degree of polymerization ≤ 7[13–17]. This is hypothesized to confer a competitive advantage to *B. infantis* in the gut of breastfed infants, allowing the subspecies to firmly establish itself in this niche. Literature suggests that different *B. infantis* strains have varying capacity to metabolize HMOs[18–20]. The prevalence of *B. infantis* in the infant gut varies depending on geographic location and cultural practices[21–23]. However, the prevalence of *B. infantis* in the infant gut microbiota has been found to be lower in many developed countries[21,23]. Prebiotics such as inulin, fructooligosaccharides, and galactooligosaccharides can improve the growth of bifidobacteria and enhance their ability to colonize the gut[24]. Yet to this date, a potential synergy between *B. infantis* and HMOs has not explicitly been shown. Recently, the concept of synbiotics has emerged, which involves combining prebiotics with probiotics to enhance the growth and activity of beneficial gut bacteria[25]. Synergistic synbiotics are a subset of synbiotics that combine a prebiotic that is specifically metabolizable by the probiotic to enhance health benefits. Still, this synergy is often challenging to

[1]Nestlé Research and Development, Nestléstrasse 3, CH-3510 Konolfingen, Switzerland. [2]Nestlé Institute of Food Safety and Analytical Science, Nestlé Research, Route du Jorat 57, CH-1000 Lausanne, Switzerland. ✉e-mail: florac.debruyn@rd.nestle.com

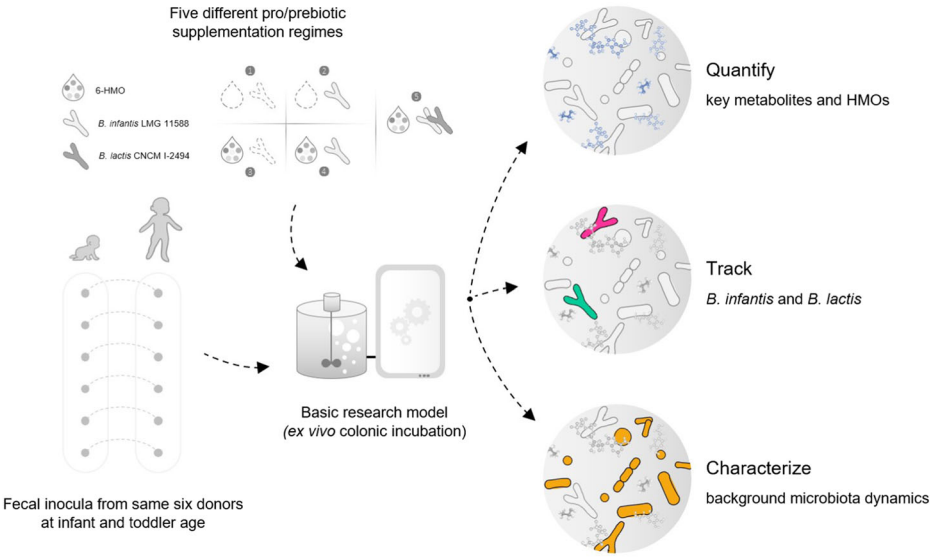

Fig. 1 | Overview of experiments and analyses performed. $n = 6$ biologically independent samples per age group. A basic research model consisting of ex vivo colonic incubation bioreactors that mimic the early life colon, seeded with cryopreserved fecal inocula, and supplemented with different pre- and probiotic combinations. Fecal inocula were harvested from the same six donors at infant (approx. 3 months old) and toddler age (approx. 12 months old). The microbiota contained in this fecal material provided a background for the system. Five different combinations of pre- and probiotics were supplemented to the bioreactors: (1) blank condition in which no prebiotic and no probiotic is added, (2) probiotic only condition in which *Bifidobacterium longum* subsp. *infantis* LMG 11588 is added, (3) prebiotic only condition in which an age-adapted human milk oligosaccharide (6-HMO) mix is added, (4) synbiotic condition in which the combination of *B. infantis* LMG 11588 and 6-HMO is added, and (5) additional probiotic supplementation condition in which *B. infantis* LMG 11588, 6-HMO, and *Bifidobacterium animalis* subsp. *lactis* CNCM I-3446 are added. Conditions 1–4 allow the methodical quantification of any potential synergy between 6-HMO and *B. infantis* LMG 11588. Condition 5 enables to assess if this synergy is influenced by additional probiotic supplementation. Triphasic analysis is performed to quantify key microbial metabolites through HPAEC and GC, to track the strains added to the system through strain-specific qPCR, and to characterize the background microbiota dynamics through 16 S rDNA sequencing.

demonstrate and quantify, especially in vivo. Therefore, we have methodically assessed the interaction and synergy between *B. infantis* and age-adapted biologically relevant HMO mixes in a well-defined ex vivo system (Fig. 1). Read-outs of this synergy include total SCFA production, HMO consumption, and microbiota dynamics. We believe our study can provide a steppingstone towards a larger in vivo study.

Results

A synergy between *Bifidobacterium longum* subsp. *infantis* LMG 11588 and HMOs increases short chain fatty acid (SCFA) production

In all conditions where the age-adapted mix of six human milk oligosaccharides (6-HMO) was supplemented, total short chain fatty acid (SCFA) production increased substantially (Fig. 2). Acetate was the main SCFA produced, followed by minor amounts of propionate, butyrate, and branched SCFAs (Fig. S1; Table S1). Unexpectedly, infant fecal donors separated into two groups based on the rate and extent of their total SCFA production (Fig. 2a). In conditions where 6-HMO was supplemented (conditions 3 and 4), three infant fecal donors (A, B, and C) showed substantial SCFA production regardless of *B. infantis* LMG 11588 supplementation. In contrast, the remaining infant donors (D, E, and F) had comparatively lower SCFA production. Indeed, sole 6-HMO supplementation resulted in a final SCFA production that was twice as high for the former group of donors compared to the latter. However, this difference in total SCFA production could be counterbalanced for donors D, E, and F by supplementing *B. infantis* LMG 11588 on top of 6-HMO (condition 4). Because of their distinctive SCFA production profiles, we will hereafter refer to donors A, B, and C as basal HMO responders since they showed a basal level of SCFA production in presence of 6-HMO. Correspondingly, we will refer to donors D, E, and F as inducible HMO responders because *B. infantis* LMG 11588 induced total SCFA production in the presence of 6-HMO. Surprisingly, the supplementation of *B. infantis* LMG 11588 on top of 6-HMOs increased total SCFA production for all infant donors (although the relative increase was largest for the inducible group). Although the difference between basal and inducible HMO responders was the clearest when solely 6-HMO was supplemented, a difference between these two groups remained clearly detectable in all infant conditions. Another distinctive feature of the infant basal HMO responders was their comparatively pronounced lactate production (Fig. S1A). For the same fecal donors at toddler age, the distinction between basal and inducible HMO responders was not found (Fig. 2b). Still, average final total SCFA production was marginally higher when *B. infantis* LMG 11588 was supplemented on top of 6-HMO compared to sole 6-HMO supplementation (46.3 mM versus 48.1 mM for basal and 43.0 mM *versus* 46.5 mM for inducible responders). The increase in total SCFA production was mainly due to *B. infantis* LMG 11588, as its growth and metabolic activity was exclusively observed in the presence of 6-HMO (Fig. S2). Analogous to total SCFA production, *B. infantis* LMG 11588 growth was more pronounced for toddlers than for infants and the difference between basal and inducible HMO responders was reduced for toddlers. Consequently, we observed a synergy between 6-HMO and *B. infantis* LMG 11588, because the combined effect of these two elements produced a result greater than could be expected from the sum of their individual contributions. This translated in a net total SCFAs increase that was larger and faster when combining 6-HMO and *B. infantis* LMG 11588 compared to the cumulated individual increases upon 6-HMO and *B. infantis* LMG 11588 supplementation. The difference in SCFA concentrations was evidently present for basal and inducible HMO responders at infant age, but resolved for toddlers. The synergy was also less apparent for toddlers in general. Subsequently, we therefore investigated if the differences in total SCFA production were based in the extent of HMO consumption.

Human milk oligosaccharide (HMO) consumption is inducible by *B. infantis* LMG 11588 supplementation for some infant donors

Fecal donors at infant age could be separated into two groups based on the rate and extent of 6-HMO consumption, as was the case for total SCFA production (Fig. 3). To substantiate the grouping of infant donors into basal and inducible responders, we performed non-metric

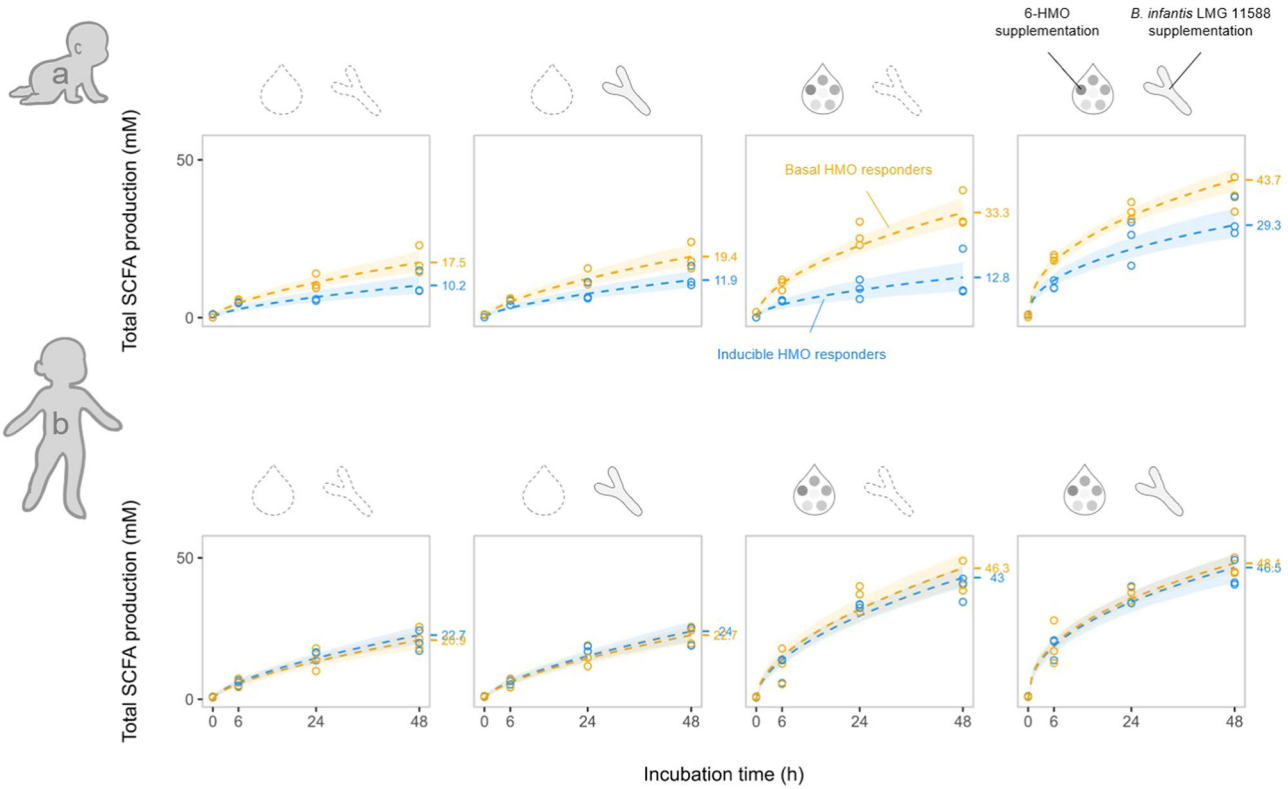

Fig. 2 | *Bifidobacterium infantis* LMG 11588 supplementation induces total short chain fatty acid production during ex vivo colonic incubation for some fecal donors and increases total short chain fatty acid (SCFA) production for all donors in combination with 6-HMO. $n = 6$ biologically independent samples per age group. Dotted lines represent the posterior means of modeled consumption profiles. Means are enveloped by a transparent ribbon representing their 95% posterior mean interval. Dots are the individual donor raw data used to fit the model. Experimental outcomes were considered meaningfully different when there was no overlap between posterior mean intervals. **a** For donors at infant age, basal total short chain fatty acid production in the absence of the age-adapted human milk oligosaccharides mix (6-HMO) was low. Upon supplementation with 6-HMO, fecal donors diverged into two groups: basal HMO responders (orange) and inducible HMO responders (blue). When *B. infantis* LMG 11588 was supplemented additionally to 6-HMO, both production rate and final SCFA production were increased for both groups. Remarkably, *B. infantis* LMG 11588 supplementation reduced the short chain fatty acid gap between basal and inducible responders. **b** For donors at toddler age, total short chain fatty acid production in the absence of 6-HMO remained relatively low. Notably, the distinction between basal and inducible responder was less pronounced for toddlers. Indeed, all toddler fecal donors showed total short chain fatty acid production in response to 6-HMO. Still, *B. infantis* LMG 11588 supplementation further increased production rate and final short chain fatty acid production for all donors when 6-HMO was supplemented.

multidimensional scaling on the modeled HMO consumption rate constants (Fig. S3). Since donors separated into the same well-defined groups, we posit that the distinction into basal and inducible HMO responder phenotypes is based on multifactorial observations. In conditions where solely 6-HMO was supplemented (in absence of *B. infantis* LMG 11588), the background gut microbiota of basal HMO responders showed rapid and complete consumption of all HMOs. By comparison, the remaining inducible HMO responders showed no or limited HMO consumption without *B. infantis* LMG 11588 supplementation. In fact, none of these infants' background gut microbiota present in the fecal inocula could metabolize all HMOs completely. Analogous to total SCFA production, HMO consumption could be induced for these infants upon supplementation of *B. infantis* LMG 11588 (Fig. 3a). Still, the rate of HMO consumption remained lower for inducible HMO responders even upon *B. infantis* LMG 11588 supplementation. HMO consumption for the same fecal donors at toddler age was very different. Indeed, toddlers' background fecal microbiota could metabolize all HMOs quickly and completely. The division between basal and inducible HMO responder phenotype was thus not observed based on HMO consumption for toddler donors, which was analogous to the total SCFA production pattern. Since we confirmed the basis for distinction into basal and inducible responders through their HMO consumption, we thereafter looked for a potential microbiota-based origin for it.

Microbiota composition associates with HMO consumption profile

To understand the HMO responder phenotype, we analyzed microbiota composition and dynamics throughout the experiments. First, we looked at the microbiota composition of the infant and toddler fecal inocula used to seed the colonic incubation bioreactors (Fig. 4). The infant fecal inocula showed marked differences in the distribution of specific bacterial taxa across basal and inducible HMO responders (Fig. 4a). Indeed, infant fecal inocula of basal HMO responders shared many more taxa compared to inducible responders. Moreover, these shared taxa were among the most prevalent in basal HMO responders and consisted of species having been described with at minimum some HMO consumption capability (*Bacteriodes* spp. and *Bifidobacterium longum*). In contrast, these taxa were below detection limits in inducible HMO responders. Toddler fecal inocula showed a considerably different microbiota profile (Fig. 4b). There, the richness and distribution of taxa was more evenly spread across basal and inducible HMO responders. Additionally, the most prevalent taxa were shared across almost all donors and were described having at minimum some HMO consumption capacity (*Bacteroides* sp., *Bifidobacterium longum*, *Bifidobacterium breve*, and *Bifidobacterium catenulatum* group). Thus, infant fecal inocula microbiota compositions mirrored the basal and inducible HMO responder phenotype distinction. At toddler age, no obvious patterns were found between responder groups, which was

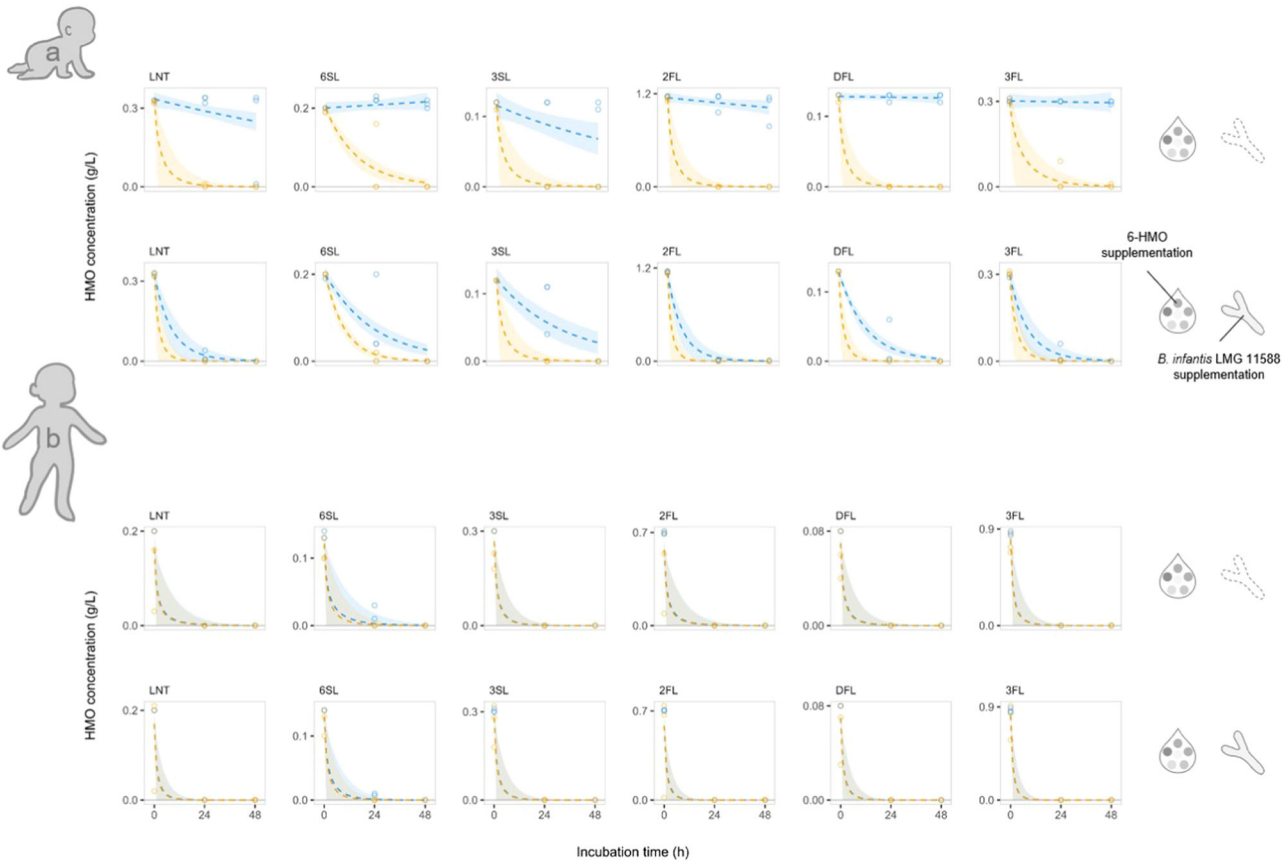

Fig. 3 | Human milk oligosaccharide consumption during ex vivo colonic incubation is determined by *Bifidobacterium infantis* LMG 11588 supplementation and age of fecal donor. Dotted lines represent the posterior means of modeled consumption profiles. $n = 6$ biologically independent samples per age group. Means are enveloped by a transparent ribbon representing their 95% posterior mean interval. Dots are the individual donor raw data used to fit the model. Experimental outcomes were considered meaningfully different when there was no overlap between posterior mean intervals. Conditions without age-adapted human milk oligosaccharides mix (6-HMO) supplementation were assessed experimentally but are omitted here for clarity since no HMOs were detected. **a** For donors at infant age without *B. infantis* LMG 11588 supplementation, a subset of donors displayed complete HMO consumption. The remaining donors did not display HMO consumption (or only very limited). However, the remaining infant donors could completely metabolize HMOs upon B. infantis LMG 11588 supplementation. The HMO consumption behavior thusly segregated donors into two groups; basal HMO responders (orange) and inducible responders (blue), mirroring the short chain fatty acid profiles (Fig. 2). **b** Remarkably, all fecal donors at toddler age could fully metabolize HMOs. Thus, the distinction between basal and inducible responders is not found for toddlers, as it was for total short chain fatty acid production.

consistent with the phenotype found for total SCFA production and HMO consumption. We also assessed the dynamics of microbiota profiles throughout the experiments to identify marker species linked to experimental conditions, fecal donor age, and responder phenotype (Fig. 5a). After controlling for incubation time, several taxa were substantially differentially present. Specifically, *Bifidobacterium infantis* was the single most prevalent taxon detected throughout experiments. Additionally, it was only detected in high abundance when both *B. infantis* LMG 11588 and 6-HMO were present together, which indicates the synergy between the two. Overall, background levels of *B. infantis* were low for fecal donors of any age and *B. infantis* LMG 11588 addition resulted in a measurable and sustained detection of a corresponding amplicon sequence variant (Fig. S4). Average microbiota α-diversity increased with longer incubation times and donor age and decreased for 6-HMO and *B. infantis* LMG 11588 addition. We also found higher average α-diversity for basal responders compared to inducible responders (Fig. S5). Microbiota β-diversity was mainly affected by incubation time and donor age, but overall, separation of samples was not clearly linked to the main factors assessed in our study (Fig. S6). We found a non-metric fit R^2 of 0.961 for the β-diversity ordination. Several co-occurrence dyads were differentially affected by experimental conditions and donor age (Fig. 5b). For conditions in which 6-HMO was not supplemented, co-occurrence between taxa was low. Upon 6-HMO supplementation in absence of *B. infantis* LMG 11588, *Bacteroides fragilis* emerged as a central taxon that co-occurred with many other taxa (*Enterococcus casseliflavius*, *Bacteroides caccae*, and *Bifidobacterium (pseudo)catenulatum/angulatum/kashiwanohense*). When supplementing 6-HMO and *B. infantis* LMG 11588, connections between *B. infantis* and multiple other taxa strengthened compared to other conditions. Strongest co-occurrences in these conditions include several *Bacteroides* spp., *Akkermansia muciniphila*, and *Alistipes finegoldii*. In general, co-occurrence between any two taxa was stronger for toddler fecal donors than for infant donors. Having found some microbiota-based differences for the HMO response phenotype, we then assessed if the synergy between *B. infantis* LMG 11588 and 6-HMO was maintained under additional probiotic supplementation.

The synergy between *B. infantis* LMG 11588 and 6-HMO is not influenced by *Bifidobacterium animalis* subsp. *lactis* CNCM I-3446

Different probiotic strains are commonly combined with the expectation that each strain will maintain its respective health benefit. To assess if an additional probiotic would influence the synergy between *B. infantis* LMG 11588 and 6-HMO, we supplemented *B. lactis* CNCM I-3446 (a probiotic with a long history of use in infants) in the synergistic condition (Fig. S7). Generally, SCFA profiles with and without *B. lactis* CNCM I-3446 did not differ fundamentally. However, final average total SCFA concentrations were higher for infant and toddler donors when *B. lactis* CNCM I-3446 was

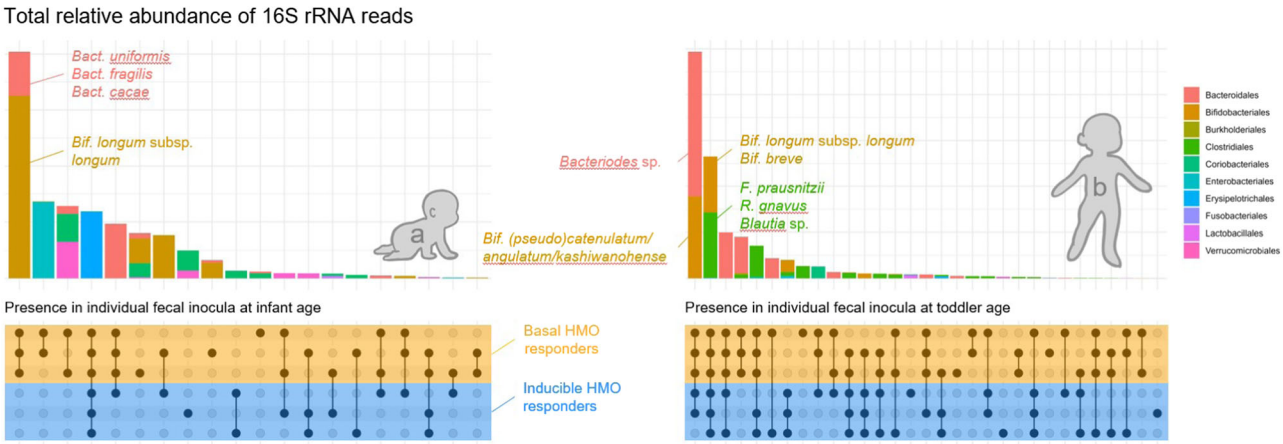

Fig. 4 | Microbiota composition of fecal inocula used for seeding of colonic incubation bioreactors show differences that can be linked to short chain fatty acids and HMO consumption. $n = 6$ biologically independent samples per age group. Vertical bars represent the summed relative abundance of taxa over infant and toddler donors, respectively. Microbial taxa identified are colored by Order-level taxonomy and ordered in decreasing order of abundance. Bottom part represents the presence of one taxon in one donor and is colored by the basal and inducible HMO response phenotype (each row represents a donor). **a** Fecal inocula of donors at infant age were less rich microbiologically and harbor stronger differences between basal and inducible HMO responders. For these donors, few taxa were shared between all donors and microbial richness is relatively low. The most abundant taxa were *Bacteriodes* spp. and *Bifidobacterium longum* subsp. *longum*. Those taxa were exclusively present in basal HMO responders and are also described as being able to metabolize HMOs. They thus represented a microbiota basis for the basal and inducible phenotype distinction at infant age. **b** Toddler fecal donors shared more taxa and harbor a larger microbial richness. Markedly, the most abundant taxa were shared by at least five out of six donors (multiple *Bifidobacterium* and *Bacteriodes* spp. as well as members of Eubacteriales). Most of these taxa have been described as able to metabolize HMOs and thus support the ubiquity of basal HMO responders for toddler fecal donors.

supplemented. Likewise, *B. lactis* CNCM I-3446 grew for some of the fecal donor conditions (especially in infant basal responders).

Discussion

Gut microbiota maturation in early life is crucial for the development of a stable and resilient microbiota. During this maturation, the dominance of bifidobacteria is nurtured by human milk oligosaccharides (HMOs) in breast milk[21,26]. Substantial research efforts are focused on understanding the synergy between *Bifidobacterium longum* subsp. *infantis* and HMOs to benefit infants that do not have (sufficient) access to human milk. Therefore, both elements of this synergy dyad need to be carefully selected. In our study, we found that this synergy was translated into a larger and faster short chain fatty acid (SCFA) production than what could be expected from the contribution of the individual dyad components, especially in infant conditions. Short-chain fatty acids (SCFAs) like acetate, propionate, and butyrate confer important health benefits and contribute to gut health, immune regulation, and brain development[27–29]. Acetate (the main SCFA produced in our study), is an energy source for intestinal cells that supports their growth and function and can even be metabolized by other bacteria in the gut (cross-feeding)[30,31]. Therefore, increasing SCFA production in vivo is of interest. The incremental advantage of a synergistic synbiotic (i.e., where the prebiotic moiety can be specifically utilized by the probiotic moiety) could be one way to leverage the full potential of both HMOs and *B. infantis*.

The delineation between basal and inducible HMO response we found appeared to be driven by the innate presence of background HMO-utilizing taxa. Observations supporting this hypothesis include the distinct presence of *Bifidobacterium longum* subsp. *longum* and *Bacteroides* spp. for basal responders and their absence in the inducible responders. Other factors like birthing method and main feeding regime at infant age did not map onto responder type unambiguously (Table S2). While *B. longum* subsp. *longum* is less associated with HMO utilization than its relative *Bifidobacterium longum* subsp. *infantis*, some strains are known to successfully metabolize HMOs due to the acquisition of HMO-utilization loci[6,32]. Some *Bacteroides* species are also known to consume a limited variety of HMOs[33]. This fits with the basal responder distinction, as it shows that these species were able to metabolize (some of) the HMOs. Their low abundance or absence in inducible responders may, in part, explain the distinct phenotypes. Remarkably, even for basal responders, supplementation of *B. infantis* LMG 11588 enhanced 6-HMO utilization, suggesting an advantage across different microbiota types. This could indicate cross-feeding of HMOs or their metabolites. Because of its intracellular feeding strategy, *B. infantis* is not as often described as a cross-feeding provider as for example *Bifidobacterium bifidum*. However, it is known to engage in some syntrophic interaction with *Bifidobacterium breve* via liberated L-fucose[5]. Moreover, fucosylated-HMO-metabolizing *Bifidobacterium* species are thought to potentially cross-feed other gut symbionts such as *Eubacterium hallii* and *Limosilactobacillus reuteri* via 1,2-propanediol generated in L-fucose metabolism[34]. In addition, this suggests that although *B. infantis* LMG 11588 prefers fucosylated HMOs it can consume all HMOs in 6-HMO, including sialylated ones, as found previously in a monoculture system[18]. Notably, the basal and inducible distinction was less pronounced for fecal donors at toddler age, as shown by SCFA production and HMO consumption. This suggests a convergent maturation of the gut microbiota throughout the transition from infancy to toddlerhood. Our study indicates that this progression is not only functional, but also representative, as specific taxa were ubiquitous across toddler donors. This is particularly the case for *Bifidobacterium*, *Bacteroides*, *Faecalibacterium*, *Ruminococcus* and *Blautia* species. Their presence suggests an acquisition of key species throughout infancy that could subsume the basal and inducible HMO responder phenotype. Given the known geographical and lifestyle-based heterogeneity in HMO profile and microbiota, it could be of value to further explore this development across diverse groups[35].

Specific inter-taxa ties were enhanced by the co-supplementation of 6-HMO and *B. infantis* LMG 11588. Specifically, we observed stronger co-occurrence of *B. infantis* with *Bacteroides fragilis*, *Bacteroides caccae*, *Alistipes finegoldii* and *Alistipes onderdonkii* in infant conditions, and with *Bacteroides eggerthi* and *Akkermansia muciniphila* in toddler conditions. Indeed, *B. infantis* appeared to play a central role in microbial network interactions. This probably links to the reduction of α-diversity we found upon *B. infantis* LMG 11588 and 6-HMO addition, as it is consistent with the effect an increase in abundance of a specific taxon would have on diversity indices accounting for both evenness and richness (Fig. S5). As *B. infantis* is shown to preferentially internalize and metabolize HMO glycans with degree of polymerization ≤ 7, it is likely largely responsible for the HMO consumption and production of compounds such as acetate, lactate, and 1,2-propanediol[13,36,37]. In turn, other co-occurrent species may benefit from cross-feeding on these generated metabolites. Indeed, 1,2-propanediol

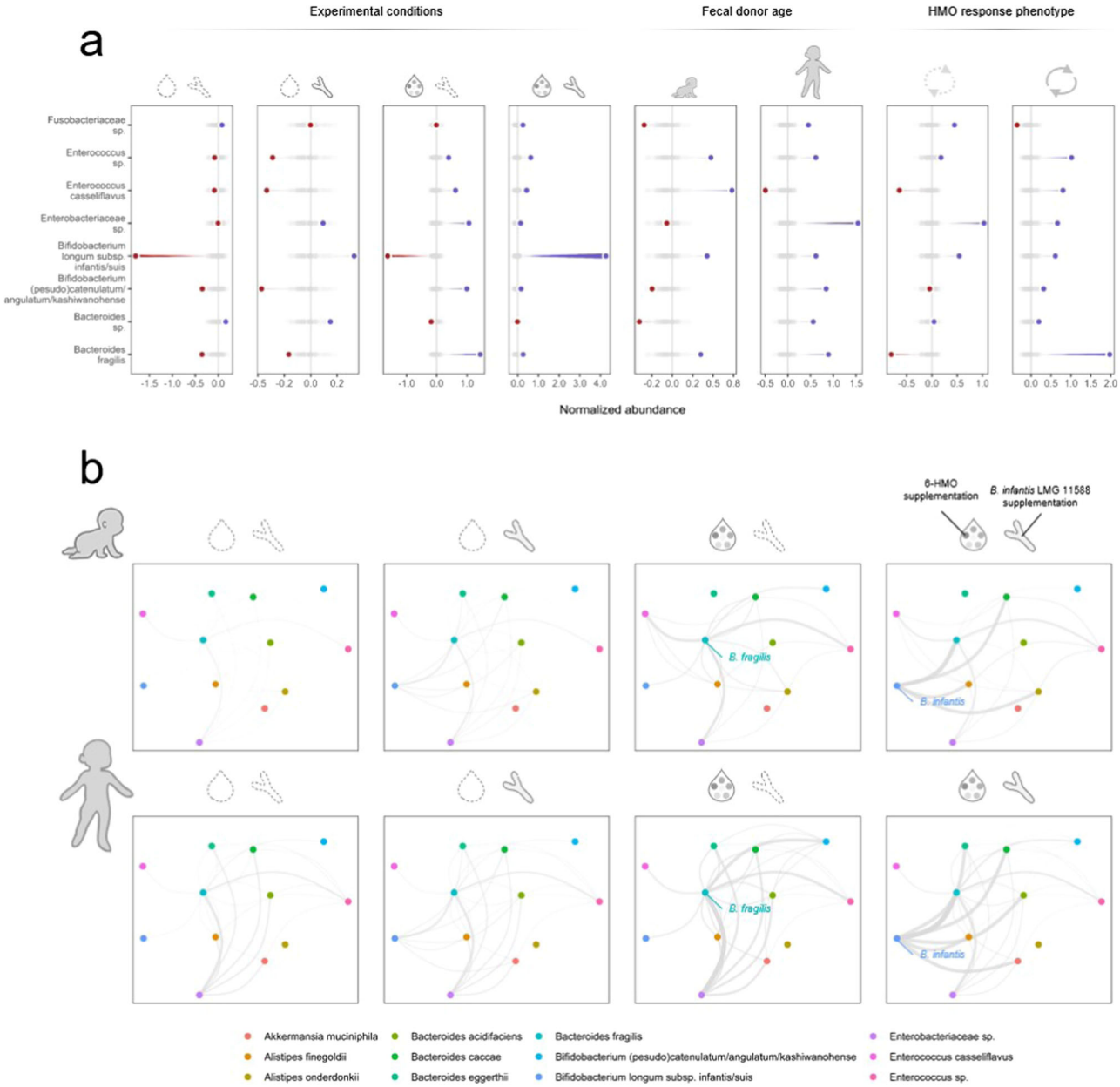

Fig. 5 | Microbiota-based differences link to age, experimental conditions, and human milk oligosaccharide response. $n = 6$ biologically independent samples per age group. **a** Maximum a posteriori estimates for experimental factor contributions to most prevalent bacterial taxa. Taxa highlighted in color as below (red) or above average (purple) compared to background taxa (represented in gray). Several taxa were substantially differentially selected for by different experimental factors. Notably, *Bifidobacterium infantis* was the single most prevalent taxon detected overall and almost exclusively so when both *Bifidobacterium infantis* LMG 11588 and 6-HMO were supplemented. When supplementing age-adapted human milk oligosaccharides mix (6-HMO) solely, differentially abundant taxa included *Bifidobacterium (pseudo)catenulatum/angulatum/kashiwanohense*, *Bacteroides fragilis*, *Enterobacteriaceae* sp., and *Enterococcus casseliflavus*. Additionally, we found *Bifidobacterium (pseudo)catenulatum/angulatum/kashiwanohense* and *Bacteroides fragilis* to be more prevalent in both basal HMO responders and toddlers. **b** Co-occurrence network of most prevalent bacterial taxa. Every node represents one of the 15 most co-occurring bacterial taxa detected by 16 S rDNA seq. The width and transparency of the edge between two nodes represent the strength of their co-occurrence. Networks are shown for infants (top row) and toddler (bottom row) fecal donors in each experimental condition. For conditions in which 6-HMO was not supplemented, co-occurrence between taxa is low. Upon 6-HMO supplementation in absence of *B. infantis* LMG 11588, Bacteroides fragilis emerged as a central taxon that co-occurred with other taxa, including *Enterococcus casseliflavius*, *Bacteroides caccae*, and *Bifidobacterium (pseudo)catenulatum/angulatum/kashiwanohense*. When supplementing 6-HMO and *B. infantis* LMG 11588 together, ties between *B. infantis* and multiple other taxa strengthened compared to other conditions. Strongest co-occurrences in these conditions included *B. fragilis*, *B. caccae*, *Bacteroides eggerthii*, *Bacteroides acifidifaciens*, *Akkermansia muciniphila*, and *Alistipes finegoldii*. In general, co-occurrence between any two taxa was stronger for toddler fecal donors than for infant donors.

is known to act as a substrate for other gut symbionts[37–39]. Moreover, some *Bacteroides* spp. are known to convert pyruvate into propionate and literature suggests that *A. muciniphila* may metabolize lactate and/or acetate to produce butyrate[40]. Although butyrate production was low in this study, its delayed production appears to substantiate this cross-feeding. Intriguingly, when 6-HMO was supplemented without *B. infantis* LMG 11588, the central node in the network was *B. fragilis*. This taxon strongly co-occurred with *Enterococcus* species and *Enterobacteriaceae* species in infants, and with *Bifidobacterium catenulatum* subspecies in toddlers. *Bacteroides fragilis* has been found able to consume HMOs (esp. 2FL, the

most abundant HMO in 6-HMO), albeit less efficiently than most infant-associated *Bifidobacterium* species[33,41].

Bacteroides spp. are thought to do so in part via membrane-bound and extracellular secreted glycoside hydrolases[42]. This mechanism is unlike *B. infantis*, which typically internalizes intact HMO glycans. This cooperative mechanism of HMO utilization by *Bacteroides* spp. may facilitate cross-feeding on small-mass HMO glycans, released via extracellular hydrolysis, by *B. catenulatum* subsp. *kashiwanohense*/*pseudocatenulatum*. While the former species are typically considered members of a healthy infant gut microbiota, some species of *Enterococcus* and *Enterobacteriaceae* are associated with infections and inflammatory disease states[43]. Additionally, bronchiolitis cases have previously been found to be more abundant in infants with *Bacteroides*-dominant microbiota[44]. This highlights the role *B. infantis* LMG 11588 may play in fostering more benevolent trophic interactions in the presence of 6-HMO, particularly in infant microbiota where bifidobacteria able to metabolize HMOs are lowly abundant or absent.

In our study, we linked the differential HMO response pattern to the reduced prevalence of HMO-metabolizing taxa in general and *B. infantis* in particular. Prevalence of *B. infantis* is typically low in infants in many developed countries, even when they are mainly breastfed[23]. An increasing number of infant formulae today are supplemented with HMOs. However, if infants do not have a microbiota capable of metabolizing these HMOs, they may miss out on benefits mediated by HMO-utilizing species. Based on literature, the low abundance of *B. infantis* for these donors is not unexpected[22,45,46]. However, it is remarkable that its abundance was enhanced so profoundly by co-supplementation of 6-HMO. Researchers have proposed that infants may obtain *B. infantis* via horizontal transfer (infant to infant) rather than vertical transfer (mother to infant)[23]. Due to the low abundance of *B. infantis* in the infant microbiota in many parts of the world, the probability of horizontal transfer is expected to decrease as well, which may amplify the loss of this relevant subspecies through a self-enforcing feedback loop. We have shown that it is possible to induce HMO consumption ex vivo through the supplementation of *B. infantis* LMG 11588. This strain was specifically selected because of its safety profile and its HMO consumption pattern. Indeed, this strain is one of the two first *B. infantis* strains isolated in the 1950s together with the type strain *B. infantis* ATCC 15697[18]. While ATCC 15697 harbors a potentially transferable resistance to streptomycin and preferentially uses lacto-N-tetraose and sialylated HMOs, LMG 11588 has no antibiotic resistance and was found to preferentially metabolize fucosylated HMOs[18]. This could represent an ecological advantage, as fucosylated HMOs are highly prevalent in human milk and make up around two thirds of both age-adapted HMO blends used in this study. The HMOs selected for the blends were representative of the main HMO classes and were present in age-adapted concentrations found in breastmilk of 0-6 months (infants) and above 6 months postpartum (toddlers)[10,11,37,47–49]. Infant formula with a similar blend of five HMOs has been found to support the development of the intestinal immune system and gut barrier function and to shift the gut microbiota closer to that of breastfed infants by increasing *B. infantis* prevalence in vivo[50]. This emphasizes the relevance of careful selection when designing synergistic synbiotics. While a lot of synbiotics can be complementary (i.e., the prebiotic cannot necessarily be metabolized by the probiotic), combining *B. infantis* and HMO into a synergistic synbiotic leverages the full potential of both moieties. Finally, we found that *B. lactis* CNCM I-3446 does not alter the synergy between 6-HMO and *B. infantis* LMG 11588. This suggests that the mechanisms of action of the synbiotic 6-HMO and *B. infantis* LMG 11588 and *B. lactis* CNCM I-3446 are independent of each other (additive) and thus do not interact regarding HMO consumption. In fact, average final SCFA concentrations were higher when *B. lactis* CNCM I-3446 was present. We posit this to be due to metabolic activity of *B. lactis* CNCM I-3446 using residual lactose in 6-HMO, as *B. lactis* is generally assumed not to be able to metabolize HMOs[14,51–54]. This is corroborated by the low-level growth of this strain we have observed here for some fecal donors. Additionally, *B. lactis* has a long history of use in infant formulae, promotes early life immune development, and improves gastrointestinal health[51–53]. In conclusion, our study uncovered two key elements. First, the existence of heterogeneity in both the composition of infant colonic microbiota and the resulting phenotype, as shown by the delineation into basal and inducible HMO responders. This distinction is apparent in total SCFA production resulting from the aptness to metabolize 6-HMO. Second, the capacity of *B. infantis* LMG 11588 to reduce differences between basal and inducible HMO responders, as shown by the synergistic increase of total SCFAs. Knowing all ex vivo basic research models have their limitations, especially regarding host interactions, a logical next step could be to confirm the synbiotic effect described in this study in an in vivo study.

Methods

Experiment design

We implemented different experimental conditions to study the interaction between human milk oligosaccharides (HMOs) and *Bifidobacterium longum* subsp. *infantis* LMG 11588 (Fig. 1). Five different combinations of pre- and probiotics were supplemented to the bioreactors: (1) blank condition in which no prebiotic and no probiotic was added, (2) probiotic only condition in which *B. infantis* LMG 11588 was added, (3) prebiotic only condition in which an age-adapted human milk oligosaccharide (6-HMO) mix was added, (4) synbiotic condition in which the combination of *B. infantis* LMG 11588 and 6-HMO was added, and (5) additional probiotic supplementation condition in which *B. infantis* LMG 11588, 6-HMO, and *Bifidobacterium animalis* subsp. *lactis* CNCM I-3446 were added. Conditions 1–4 allowed the methodical quantification of any potential synergy between 6-HMO and *B. infantis* LMG 11588. Condition 5 enabled to check if this synergy is robust to additional probiotic supplementation.

Ex vivo colonic incubations

Unless mentioned differently, all medium components and reagents used were purchased from Merck KGaA (Darmstadt, Germany). Short-term single-stage colonic simulator of the human intestinal microbial ecosystem (SHIME) experiments simulating only the proximal large intestine were performed by ProDigest (Ghent, Belgium) as described before[55]. This simplified model is commonly used to study ingredients that are expected to arrive in the colon and that are expected to exert their benefits in the colon such as prebiotics and probiotics. Fecal material of the same six donors at infant age and toddler age was used to seed the ex vivo colonic incubation bioreactors (Table S2). Fecal material was collected according to the ethical approval of the University Hospital Ghent (reference number B670201836585). Informed consent of legal representatives was obtained after providing them with detailed information about the project and the use of the samples. All ethical regulations relevant to human research participants were followed. Fecal material was cryopreserved at −80 °C immediately after collection as described before[56]. SHIME colonic background medium containing basal nutrients that are present in the colon (K_2HPO_4 4.7 g/L; KH_2PO_4 14.7 g/L; $NaHCO_3$ 1.8 g/L; yeast extract 1.8 g/L; peptone 1.8 g/L; mucin 0.9 g/L; cysteine 0.5 g/L; polyoxyethylene sorbitan monooleate 20 1.8 mL/L) were used in all experiments and 1 mL of fecal inoculum was added to 63 mL colonic background medium[57]. Incubation vessels were kept under anaerobic atmosphere through N_2 flushing, shaken at 90 rpm, controlled at 37 °C, and ran for 48 h. When not processed immediately, samples were filtered and frozen at −80 °C before analysis.

Bifidobacterium longum subsp. *infantis* LMG 11588 and *Bifidobacterium animalis* subsp. *lactis* CNCM I-3446 biomass production

Biomass for all experiments was produced on culture medium containing glucose, yeast extract, and sodium ascorbate[55]. Biomass production was carried out in the 1-L Eppendorf DASGIP Parallel Bioreactor System (Hamburg, Germany) under anaerobic conditions at 37 °C and with pH control at 6.0. Anaerobic conditions were maintained by flushing the headspace with carbon dioxide. The inoculation level was 10^7 CFU/mL. Fermentations were stopped in the stationary growth phase, biomass was harvested via

centrifugation, washed with phosphate buffered saline, and immediately cryopreserved at −80 °C with 15% w/w glycerol as a cryoprotectant. Inoculation levels were targeted at 1.0×10^8 CFU/mL for each strain at the start of ex vivo colonic incubations.

Human milk oligosaccharides mixture (6-HMO)

A specific HMO mix was designed for the experimental infant and toddler ex vivo conditions. Both mixes consisted of the same 6 HMOs representing the major classes of HMOs found in human milk. Powder-form HMOs were obtained from Glycom A/S (Hørsholm, Denmark). Individual HMO concentrations were equal or above the fifth percentile of concentrations for the same HMOs measured in breastmilk for 0-6 months (infants) and above 6 months of lactation (toddlers)[10,11,37,47–49]. Only mature breast milk data (> 21 days postpartum) was considered. The HMOs in the mix consisted of (dry HMO wt/wt) 13.5% 3'-fucosyllactose (3FL), 50.1% 2'-fucosyllactose (2FL), 5.9% difucosyllactose (DFL), 6.0% 3'-sialyllactose (3SL), 8.2% 6'-sialyllactose (6SL), and 16.3% lacto-N-tetraose (LNT) for infants and 37.4% 3'-fucosyllactose (3FL), 29.3% 2'-fucosyllactose (2FL), 3.4% difucosyllactose (DFL), 14.4% 3'-sialyllactose (3SL), 5.3% 6'-sialyllactose (6SL), and 10.2% lacto-N-tetraose (LNT) for toddlers. The HMO mix was added at a level of 2.5 g total HMO/L to the ex vivo colonic incubators. Residual lactose content in the HMO mix was < 5% dry wt/wt.

Microbiological analyses

16 S rDNA gene amplicon sequencing, bioinformatic analysis, and flow cytometry

DNA of triplicate samples for each biological replicate was extracted as described before[58]. DNA was extracted from fecal donor inocula and from bioreactor liquid after 0, 24, and 48 h of incubation. DNA extracts were sent out to LGC Genomics, GmbH (Teddington, UK) for 16 S rDNA gene PCR targeting the V3-V4 region with the 341 F (5′-CCTACGGGNGGCWGCAG-3′) and the modified 785 R (5′-GACTACHVGGGTATCTAAKCC-3′) primers as described before[59]. Quality control of the PCR products was done using the Fermentas PCR Kit according to the manufacturer's instructions (Thermo Fisher Scientific, Inc.; Waltham, Massachusetts, USA) and sequence length distribution was verified by electrophoresis on a 2% (w/v) agarose gel for 30 min at 100 V. The PCR products were sequenced on the 2 ×250 bp MiSeq platform (Illumina, Inc; San Diego, California, USA) according to the manufacturer's standard protocol. Reads were converted into amplicon sequence variants (ASVs) using DADA2 version 1.15.2 with following filtering parameter values; truncLen = c(0,0), truncQ = 2, maxN = 0, and maxEE = c(2,2)[60]. Genus level taxonomy was assigned to ASVs using a naïve Bayesian classifier and the SILVA ribosomal RNA gene database version 132[61]. Species-level taxonomy was assigned using highest identity BLASTN hit in NCBI's type material-restricted nucleotide collection database and cross-checked with the SILVA ribosomal RNA gene database where possible[62,63]. Where possible, we assigned subspecies level identification for Bifidobacterium based on the signatures on SILVA aligned 16 S rDNA as described before[64]. Adequate sequencing depth was checked by making sure sample rarefaction curves showed a distinct plateau. Total cell densities were determined using a CytoFLEX V2-B4-R2 flow cytometer (Beckman Coulter Life Sciences; Brea, California, US) with the PI/Syto 24 method as described in standard ISO 19344:2015[65]. The proportion of each ASV obtained through 16 S rDNA gene amplicon sequencing was multiplied by the total cell counts obtained through flow cytometry to obtain absolute cell numbers for each ASV. During this analysis, we made the conscious decision not to correct for gene copy number or amplification bias, because the implementation of this correction is highly complex and its potential added value to our specific study is minimal.

Strain-specific qPCR assay. All oligonucleotides and consumables for qPCR were ordered from Thermo Fisher Scientific (Waltham, Massachusetts, US). Probes were labeled with a FAM fluorophore and a BHQ-QSY quencher. A qPCR assay with forward primer TCCAAACGAGATACGTAATAAAATGG, reverse primer CCTTATTAGCCGCCCTTTGC, and Taqman probe FAM-TCGCCATTCTCCAACCCTGTCCG-BHQ-QSY was designed to target *B. infantis* LMG 11588. *Bifidobacterium lactis* CNCM I-3446 was targeted with forward primer CTGAGAAGAGCCCCTAAATCATG, reverse primer GGGATGCCACACTAGCGAAA, and Taqman probe FAM-ATGCCCGCAAGGAACACAGTGACC-BHQ-QSY. Real-time PCR runs were performed on a Quantstudio 5 (Thermo Fisher Scientific), equipped with a 384-well block. Each sample was analyzed in triplicate. DNA was extracted from fermentate as described before[66]. Reactions consisted of a 10 µL amplification mix containing 1 ng of sample DNA, 2 µL of 5X LightCycler® Multiplex DNA Mastermix, 1 µL of 10X IPC mix, 0.5 µL of 50X IPC DNA, 200 nM and 100 nM of each primer and probe, respectively. The following cycling program was applied: pre-incubation for 5 min at 95 °C and ramp rate 4.8 °C/s, 40 amplification cycles for 10 s at 95 °C and ramp rate 4.8 °C/s followed by 30 s at 60 °C and ramp rate 2.5 °C/s, and final cooling for 30 s at 40 °C and ramp rate 2.5 °C/s. The specificity of both assays was checked against other selected *Bifidobacterium* strains deposited in the Nestlé Culture Collection (Nestlé Research, Lausanne, Switzerland; Table S3).

Short-chain fatty acid and lactic acid quantification

Short and branched chain fatty acids (acetate, propionate, butyrate, valerate, iso-butyrate and iso-valerate) were quantified using a solid phase microextraction gas chromatography coupled to mass spectrometry (SPME-GC-MS, Agilent; Santa Clara, California, USA) as described previously with minor modifications[67]. Briefly, 50 µL of samples were stabilized with 0.5% ortho-phosphoric acid, labeled internal standards ($^2H_3$-acetic acid, $^2H_5$-propionic acid, $^2H_5$-butyric acid, $^2H_7$-isobutyric acid, $^2H_9$-valeric acid, and $^2H_9$-isovaleric acid) were added and vortexed gently. The SPME-GC-MS conditions were as follows: PDMS/DVB fiber (Supelco; Bellefonte, Pennsylvania, USA), agitation at 40 °C with an extraction time of 10 min. Temperature and time of desorption were set at 250 °C for 5 min. The GC conditions were as follows: inlet temperature at 250 °C with as carrier gas. The temperature program was 100 °C for 4 min, followed by an increase to 240 °C at 11 °C/min for a total time of approx. 16.7 min. Calibration curves were made by plotting ratio between each metabolite and their respective internal standard peak areas against the theoretical standard concentration. The concentrations were then determined with a linear regression model with a weighted x^{-1} model. Repeatability and intermediate reproducibility (coefficient of variation) were lower than 15% for all the metabolites measured.

Human milk oligosaccharide quantification

Human milk oligosaccharides were quantified through ultra-high performance liquid chromatography with fluorescent detection as described before[37]. In short, supernatants from bioreactors were rendered cell-free through centrifugation and filtration and cryopreserved at -80 °C. At the time of analysis, supernatants were thawed and human milk oligosaccharides were labeled with a fluorescent tag (2-aminobenzamide) before quantification.

Statistics and reproducibility

All modeling was implemented in a fully Bayesian framework. Where not explicitly stated, statistics were calculated using R version 3.6.3 base functions[68]. Unless stated otherwise, reported values are averages of technical triplicates. The models described below were fitted in RStan version 2.21.2 and sampled though Hamiltonian Markov chain Monte Carlo[69]. Unless stated otherwise, reported quantities after modeling are posterior means. Prior predictive simulation was performed to define priors limiting the outcome space to the scientifically possible range. Where needed, non-centered parametrization was used to optimize sampling. Convergence and efficiency diagnostics were checked by visual inspection of trace and rank plots. All model parameters had R-hat ≤ 1.01 and effective sample size ≥

1000. Highest continuous 95% density intervals based on 1000 samples are represented as shaded areas with a dotted overlay for the posterior mean. Differences between were considered meaningful when there was no overlap between 95%-posterior mean intervals.

Modeling combined total short chain fatty acid production and consumption

Because total short chain fatty acid levels are determined by simultaneous production and consumption at potentially different rates, we modeled its evolution through linear combination of both processes in the rethinking package version 2.13[70]. Production and consumption of short chain fatty acids was modeled as

$$\triangle c = \alpha t^{\beta} - \gamma c \Longleftrightarrow c = \frac{\alpha t^{\beta}}{\gamma + 1} \quad (1)$$

in which c is the concentration of total fatty acids scaled between (0,1), α is the production rate, t is incubation time in h, β is a diminishing return (elasticity) constant, and γ is the consumption rate. Next, c was assigned a Gaussian likelihood with its mean determined by Eq. (2), that is;

$$c \sim Normal\left(\bar{\mu}, \bar{\sigma}\right)$$

$$\bar{\mu} = \frac{\alpha t^{\beta}}{\gamma + 1}$$

$$\bar{\sigma} \sim Exponential(1).$$

Model parameters were as follows;

$$\alpha = \alpha_0[\text{condition}] + \alpha_1\left[\text{condition}, \text{age}\right] + \alpha_2\left[\text{condition}, \text{group}\right] + \alpha_3\left[\text{age}, \text{group}\right]$$

$$\alpha_0[\text{condition}] \sim HalfNormal(0,\ 0.5)$$

$$\alpha_{1,2,3}\left[i, j\right] \sim MVNormal(0, \Sigma)$$

with $\Sigma = \sigma\rho\sigma^{T}$, $\sigma \sim Exponential(1)$, and $\rho \sim LKJcorr(2)$

$$\beta = \beta_0[\text{condition}]$$

$$\beta_0[\text{condition}] \sim Normal(1,\ 0.1)$$

$$\gamma = \gamma_0[\text{condition}]$$

$$\gamma_0[\text{condition}] \sim Exponential(1),$$

in which any parameter with structure *X[i,j]* is a matrix with all levels of *i* as rows and all levels of *j* as columns, Σ is a covariance matric Cholesky decomposed into $\sigma\rho\sigma^{T}$, the vector *condition* contains all levels of experimental conditions, the vector *age* contains all levels of donor age, and the vector *group* contains a grouping variable for spontaneous HMO responders (donors A, B, C) and HMO non-responders (donors D, E, F).

Modeling *Bifidobacterium infantis* LMG 11588 copies progression (strain-specific qPCR)

Copy progression for *B. infantis* LMG 11588 were modeled in brms version 2.16.1 package using a Gaussian process because of the flexibility it provides and the non-stringent assumptions it allows when applied on relatively little data[71]. Copy numbers were modeled for each unique condition/age/group combination z as

$$c_z = \alpha_z + f_z(t)$$

in which c_z is the concentration of copies/mL scaled between (0,1). Model parameters were as follows;

$$\alpha_z \sim Student(3,\ 0,\ 2.5)$$

$$f_z(t) \sim MVNormal(0, k_z(t))$$

$$\text{with } k_z\left(t_i, t_j\right) = \text{sdgp}_z^{\,2} e^{\frac{-\|t_i - t_j\|^2}{2\,\text{lscale}_z^{\,2}}} \text{ for all possible points i, j within z}$$

in which $\text{sdgp}_z \sim Student(3,\ 0,\ 2.5)$ and $\text{lscale}_z \sim InvGamma(46,\ 31)$.

Modeling HMO consumption

Since HMOs can only be consumed and at no time produced, we modeled their consumption via exponential decay in the rethinking package version 2.13[70]. The concentration decrease of HMOs was modeled with a Gaussian likelihood with its mean determined by exponential decay, that is for each HMO;

$$c \sim Normal\left(\bar{\mu}, \bar{\sigma}\right)$$

$$\bar{\mu} = \alpha e^{-\beta t} \quad (2)$$

$$\bar{\sigma} \sim Exponential(1),$$

in which c is the concentration of each HMO in g/L scaled between (0,1) and t is the incubation time in h. Model parameters were as follows;

$$\alpha = \alpha\left[\text{condition}, \text{age}\right] \sim MVNormal(0, \Sigma)$$

$$\text{with } \Sigma = \sigma\rho\sigma^{T}, \sigma \sim Exponential(1), \text{ and } \rho \sim LKJcorr(2)$$

$$\beta = \beta_0[\text{condition}] + \beta_1\left[\text{group}, \text{age}\right]$$

$$\beta_0[\text{condition}] \sim HalfNormal(0,\ 0.1)$$

$$\beta_1\left[\text{group}, \text{age}\right] \sim MVNormal(0, \Sigma)$$

$$\text{with } \Sigma = \sigma\rho\sigma^{T}, \sigma \sim Exponential(1), \text{ and } \rho \sim LKJcorr(2),$$

in which any parameter with structure *Θ[i,j]* is a matrix with all levels of *i* as rows and all levels of *j* as columns, Σ is a covariance matric Cholesky decomposed into $\sigma\rho\sigma^{T}$, the vector *condition* contains all levels of experimental conditions, the vector *age* contains all levels of donor age, and the vector *group* contains a grouping variable for spontaneous HMO responders (donors A, B, C) and HMO non-responders (donors D, E, F).

Modeling microbiota differences linked to experimental conditions

We obtained taxa-specific cell densities by mapping the relative abundances obtained through 16 S rDNA sequencing onto the total cell number obtained through flow cytometry. Cell densities were transformed by subtracting their grand mean and dividing by their standard deviation to obtain a variable with mean of 0 and standard deviation of 1. The cell density for each bacterial taxon was modeled with a Gaussian likelihood with its mean determined by decoupled contributions for each experimental factor in the

rethinking package version 2.13[70]. That is

$$N \sim Normal(\bar{\mu}, \bar{\sigma})$$

$$\bar{\mu} = \alpha_1[\text{condition, taxon}] + \alpha_2[\text{age, taxon}] + \alpha_3[\text{responder, taxon}] + \alpha_4[\text{time, taxon}]$$

$$\alpha_{1,2,3,4}[i, j] \sim Normal(0, 1)$$

$$\bar{\sigma} \sim Exponential(1).$$

in which any parameter with structure *X[i,j]* is a matrix with all levels of *i* as rows and all levels of j as columns and represents the contribution of experimental factor *i* for taxon *j*.

Modeling taxa co-occurrence

A continuous co-occurrence metric $x_{i,j}$ for experimental condition *i* and fecal donor age *j* between taxon *A* and taxon *B* was modeled as follows

$$x_{i,j} = \begin{cases} 0 \; \forall \, N_{A,i,j} = 0 \; or \; N_{B,i,j} = 0 \\ \frac{N_{A,i,j} + N_{B,i,j}}{2} \; \forall N_{A,i,j} \neq 0 \; and \; N_{B,i,j} \neq 0 \end{cases}$$

Where $N_{A,i,j}$ and $N_{A,i,j}$ are the summed cell densities in condition *i* and age group *j* for taxon A and B, respectively. Co-occurrences values were then scaled between (0,1). A co-occurrence network using the Kamada-Kawai layout was plotted using ggraph version 2.0.5[72].

Non-metric multidimensional scaling and diversity index calculation

To assess differences in HMO response profile between individual donors, non-metric multidimensional scaling (NMDS) was performed on the posterior mean of decay rate parameter β obtained in Eq. (2) using the Euclidean distance and vegan version 2.5-6[73] To assess the effect of incubation time, HMO mix addition, *B. infantis* LMG 11588 addition, donor identification, donor age, and HMO responder type on β diversity, NMDS was performed on the 16 S rDNA seq reads on the Bray-Curtis distance in the same way. To assess the effect of the same factors on α diversity, Shannon and Simpson diversity indices were calculated using the same R package.

Reporting summary

Further information on research design is available in the Nature Portfolio Reporting Summary linked to this article.

Data availability

The datasets generated during and/or analysed in the current study are available from the corresponding author on reasonable request. The 16 S rDNA sequencing data used in this study have been deposited in the European Nucleotide Archive under accession numbers ERX11887871-ERX11888086 in project PRJEB71952. Source data used for Fig. S1 are available in Supplementary Data 1. Processed 16 S rRNA gene sequencing data used for Figs, S4–6 are available in Supplementary Data 2

Received: 30 January 2024; Accepted: 24 July 2024;
Published online: 04 August 2024

References

1. Vallès Y. et al. Microbial succession in the gut: Directional trends of taxonomic and functional change in a birth cohort of spanish infants. *PLoS Genet* **10**, e1004406 (2014).
2. Hill, C. J. et al. Evolution of gut microbiota composition from birth to 24 weeks in the INFANTMET Cohort. *Microbiome* **5**, 4 (2017).
3. Turroni, F. et al. Diversity of bifidobacteria within the infant gut microbiota. *PLOS ONE* **7**, 5 (2012).
4. Roger, L. C., Costabile, A., Holland, D. T., Hoyles, L. & McCartney, A. L. Examination of faecal *Bifidobacterium* populations in breast- and formula-fed infants. *Microbiology* **156**, 3329–3341 (2010).
5. Ojima, M. N. et al. Priority effects shape the structure of infant-type *Bifidobacterium* communities on human milk oligosaccharides. *ISME J.* **16**, 2265–2279 (2022).
6. Lawson, M. A. E. et al. Breast milk-derived human milk oligosaccharides promote *Bifidobacterium* interactions within a single ecosystem. *ISME J.* **14**, 635–648 (2020).
7. Underwood, M. A., German, J. B., Lebrilla, C. B. & Mills, D. A. Bifidobacterium longum subspecies infantis: champion colonizer of the infant gut. *Pedriatic Res.* **77**, 229–235 (2015).
8. Insel, R. & Knip, M. Prospects for primary prevention of type 1 diabetes by restoring a disappearing microbe. *Pediatr. Diab.* **18**, 1400–1406 (2018).
9. Garrido, D., Barile, D. & Mills, D. A molecular basis for bifidobacterial enrichment in the infant gastrointestinal tract. *Adv. Nutr.* **3**, 415–421 (2012).
10. Austin, S. et al. Temporal change of the content of 10 oligosaccharides in the milk of Chinese urban mothers. *Nutrients* **8**, 436 (2016).
11. Plows, J. et al. Longitudinal Changes in Human Milk Oligosaccharides (HMOs) Over the Course of 24 Months of Lactation. *J. Nutr.* **151**, 876–882 (2021).
12. Mainardi, F. et al. Human milk oligosaccharide composition and associations with growth: results from an observational study in the US. *Front. Nutr.* **10**, 1–15 (2023).
13. LoCascio, R. G. et al. Glycoprofiling of bifidobacterial consumption of human milk oligosaccharides demonstrates strain specific, preferential consumption of small chain glycans secreted in early human lactation. *J. Agric. Food Chem.* **55**, 8914–8919 (2007).
14. Sela, D. Bifidobacterial utilization of human milk oligosaccharides. *Int. J. Food Microbiol.* **149**, 58–64 (2011).
15. Zabel, B. E. et al. Strain-specific strategies of 2′-fucosyllactose, 3-fucosyllactose, and difucosyllactose assimilation by *Bifidobacterium longum* subsp. *infantis* Bi-26 and ATCC 15697. *Sci. Rep.* **10**, 15919 (2020).
16. LoCascio, R. G., Desai, P., Sela, D. A., Weimer, B. & Mills, D. A. Broad conservation of milk utilization genes in *Bifidobacterium longum* subsp. *infantis* as revealed by comparative genomic hybridization. *Appl. Environ. Microbiol.* **76**, 7373–7381 (2010).
17. Sela, D. A. et al. The genome sequence of *Bifidobacterium longum* subsp. *infantis* reveals adaptations for milk utilization within the infant microbiome. *Proc. Natl Acad. Sci. USA* **105**, 18964–18969 (2008).
18. Duboux, S., Ngom-Bru, C., De Bruyn, F. & Bogicevic, B. Phylogenetic, functional and safety features of 1950s *B. infantis* Strains,». *Microorganisms* **10**, 203 (2022).
19. Zabel, B. et al. Novel Genes and Metabolite Trends in *Bifidobacterium longum* subsp. *infantis* Bi-26 Metabolism of Human Milk Oligosaccharide 2′-fucosyllactose. *Sci. Rep.* **9**, 7983 (2019).
20. Capeding, M. R. Z. et al. Safety, efficacy, and impact on gut microbial ecology of a *Bifidobacterium longum* subspecies *infantis* LMG11588 supplementation in healthy term infants: a randomized, double-blind, controlled trial in the Philippines. *Front. Nutr.* **14**, 1319873 (2023).
21. Olm, M. et al. Robust variation in infant gut microbiome assembly across a spectrum of lifestyles. *Science* **10**, 1220–1223 (2022).
22. Vatanen, T. et al. A distinct clade of *Bifidobacterium longum* in the gut of Bangladeshi children thrives during weaning. *Cell* **185**, 4280–4297 (2022).
23. Thaft, D. et al. *Bifidobacterium* Species colonization in infancy: a global cross-sectional comparison by population history of breastfeeding. *Nutrients* **14**, 1423 (2022).

24. Vandeplas, Y., Zakharova, I. & Dmitrieva, Y. Oligosaccharides in infant formula: more evidence to validate the role of prebiotics. *Br. J. Nutr.* **113**, 1339–1344 (2015).
25. Swanson, K. S., Gibson, G. R., Hutkins, R. & Reimer, R. A. The International Scientific Association for Probiotics and Prebiotics (ISAPP) consensus statement on the definition and scope of synbiotics. *Nat. Rev. Gastroenterol. Hepatol.* **17**, 687–701 (2020).
26. Matsuki, T. et al. A key genetic factor for fucosyllactose utilization affects infant gut microbiota development. *Nat. Commun.* **7**, 11939 (2016).
27. Smith, P. et al. The microbial metabolites, short-chain fatty acids, regulate colonic Treg cell homeostasis. *Sience* **341**, 569–573 (2013).
28. Holscher, H. Dietary fiber and prebiotics and the gastrointestinal microbiota. *Gut Microbes* **8**, 172–184 (2017).
29. Silva, Y., Bernardi, A. & Frozza, R. The role of short-chain fatty acids from gut microbiota in gut-brain communication. *Front. Endocrinol.* **11**, 25 (2020).
30. Vanegas, D. P. et al. Short chain fatty acids (SCFAs)-mediated gut epithelial and immune regulation and its relevance for inflammatory bowel diseases. *Front. Immunol.* **10**, 1–16 (2019).
31. Culp, E. J. & Goodman, A. L. Cross-feeding in the gut microbiome: ecology and mechanisms. *Cell Host Microbe* **31**, 485–499 (2023).
32. Garrido, D. et al. A novel gene cluster allows preferential utilization of fucosylated milk oligosaccharides in *Bifidobacterium longum* subsp. *longum* SC596. *Sci. Rep.* **6**, 35045 (2016).
33. Yu, Z., Chen, C. & Newsburg, D. Utilization of major fucosylated and sialylated human milk oligosaccharides by isolated human gut microbes. *Glycobiology* **23**, 1281–1292 (2013).
34. Bunesova, V., Lacroix, C. & Schwab, C. Fucosyllactose and L-fucose utilization of infant *Bifidobacterium longum* and *Bifidobacterium kashiwanohense*. *BMC Microbiol.* **16**, 248 (2016).
35. Marcobal, A. et al. *Bacteroides* in the infant gut consume milk oligosaccharides via mucus-utilization pathways. *Cell Host Microbe* **10**, 507–514 (2011).
36. Dedon, L., Özcan, E., Rani, A. & Sela, D. *Bifidobacterium infantis* metabolizes 2′fucosyllactose-derived and free fucose through a common catabolic pathway resulting in 1,2-propanediol secretion. *Front. Nutr.* **7**, 583397 (2020).
37. Schwab, C. et al. Trophic Interactions of infant bifidobacteria and *Eubacterium hallii* during L-fucose and fucosyllactose degradation. *Front. Microbiol.* **8**, 95 (2017).
38. Cheng, C. et al. Ecological importance of cross-feeding of the intermediate metabolite 1,2-propanediol between bacterial gut symbionts. *Appl. Environ. Microbiol.* **86**, e00190–20 (2020).
39. Engels, C., Ruscheweyh, H., Beerenwinkel, N., Lacroix, C. & Schwab, C. The common gut microbe *Eubacterium hallii* also contributes to intestinal propionate formation. *Front. Microbiol.* **7**, 713 (2016).
40. Imdad, S., Lim, W., Kim, J. & Kang, C. Intertwined relationship of mitochondrial metabolism, gut microbiome and exercise potential,». *Int. J. Mol. Sci.* **23**, 2679 (2022).
41. Martin, F. et al. Host–microbial co-metabolites modulated by human milk oligosaccharides relate to reduced risk of respiratory tract infections. *Front. Nutr.* **9**, 935711 (2022).
42. Marcobal, A. & Sonnenburg, J. Human milk oligosaccharide consumption by intestinal microbiota. *Clin. Microbiol. Infect.* **18**, 12–15 (2012).
43. Beldelli, V., Scaldaferri, F., Putignani, L. & Del Chierico, F. The role of enterobacteriaceae in gut microbiota dysbiosis in inflammatory bowel diseases. *Microorganisms* **9**, 697 (2021).
44. Hasegawa, K. et al. Sphingolipid metabolism potential in fecal microiome and bronchiolitis in infants: a case-control study. *BMC Res. Notes* **10**, 325 (2017).
45. Lefebvre, G. et al. Time of lactation and maternal fucosyltransferase genetic polymorphisms determine the variability in human milk oligosaccharides. *Front. Nutr.* **7**, 574459 (2020).
46. Austin, S. et al. Human milk oligosaccharides in the milk of mothers delivering term versus preterm infants. *Nutrients* **11**, 1182 (2019).
47. Samuel, T. et al. Impact of maternal characteristics on human milk oligosaccharide composition over the first 4 months of lactation in a cohort of healthy European mothers. *Sci. Rep.* **9**, 11767 (2019).
48. Sprenger, N., Lee, L., De Castro, C., Steenhout, P. & Thakkar, S. Longitudinal change of selected human milk oligosaccharides and association to infants' growth, an observatory, single center, longitudinal cohort study. *PLoS One* **12**, e0171814 (2017).
49. Austin, S. & Bénet, T. Quantitative determination of non-lactose milk oligosaccharides. *Anal. Chim. Acta* **10**, 86–96 (2018).
50. Bosheva, M. et al. & 5 HMO Study Investigator Consortium. Infant formula with a specific blend of five human milk oligosaccharides drives the gut microbiota development and improves gut maturation markers: a randomized controlled trial. *Front. Nutr.* **9**, 920362 (2022).
51. Mohan, R. et al. Effects of *Bifidobacterium lactis* Bb12 supplementation on body weight, fecal pH, acetate, lactate, calprotectin, and IgA in preterm infants. *Pediatr. Res.* **64**, 418–422 (2008).
52. Chouraqui, J., Van Egroo, L. & Fichot, M. Acidified milk formula supplemented with *Bifidobacterium lactis*: impact on infant diarrhea in residential care settings. *J. Pediatr. Gastroenterol. Nutr.* **38**, 288–292 (2004).
53. Weizman, Z., Asli, G. & Alsheikh, A. Effect of a probiotic infant formula on infections in child care centers: comparison of two probiotic agents. *Pediatrics* **115**, 5–9 (2005).
54. Sela, D. & Mills, D. Nursing our microbiota: molecular linkages between bifidobacteria and milk oligosaccharides. *Trends Microbiol.* **18**, 298–307 (2010).
55. Marsaux, B. et al. Synbiotic effect of Bifidobacterium lactis CNCM I-3446 and bovine milk-derived oligossacharides on infant gut microbiota. *Nutrients* **12**, 2268 (2020).
56. Hoefman, S., Pommerening-Röser, A., Samyn, E., De Vos, P. & Heylen, K. Efficient cryopreservation protocol enables accessibility of a broad range of ammonia-oxidizing bacteria for the scientific community. *Res. Microbiol.* **164**, 288–292 (2013).
57. Molly, K., Vande Woestyne, M. & Verstraete, W. Development of a 5-step multichamber reactor as a simulation of the human intestinal microbial ecosystem. *Appl. Microbiol. Biotechnol.* **39**, 254–258 (1993).
58. De Paepe, K., Kerckhof, F. M., Verspeet, J., Courtin, C. M. & Van de Wiele, T. Inter-individual differences determine the outcome of wheat bran colonization by the human gut microbiome. *Environ. Mircrobiol.* **19**, 3251–3267 (2017).
59. Klindworth, A. et al. Evaluation of general 16S ribosomal RNA gene PCR primers for classical and next-generation sequencing-based diversity studies. *Nucleic Acids Res.* **41**, e1 (2013).
60. Callahan, B. J. et al. DADA2: High-resolution sample inference from Illumina amplicon data. *Nat. Methods* **13**, 581–583 (2016).
61. Quast, C. et al. The SILVA ribosomal RNA gene database project: improved data processing and web-based tools. *Nucleic Acids Res.* **41**, D590–D596 (2013).
62. Altschul, S. F., Gish, W., Miller, W., Meyers, E. W. & Lipman, D. J. Basic local alignment search tool. *J. Mol. Biol.* **215**, 403–410 (1990).
63. [Online]. Available: https://blast.ncbi.nlm.nih.gov/Blast.cgi?PAGE_TYPE=BlastSearch. Accessed on April 20, 2022.
64. Kieser, S. et al. Bangladeshi children with acute diarrhoea show faecal microbiomes with increased *Streptococcus* abundance, irrespective of diarrhoea aetiology. *Environ. Microbiol.* **20**, 2256–2269 (2018).
65. International Dairy Federation, *Milk and milk products — Starter cultures, probiotics and fermented products — Quantification of lactic acid bacteria by flow cytometry*, International Organization for Standardization (2015).
66. Boon, N., Top, E., Verstraete, W. & Siciliano, S. Bioaugmentation as a tool to protect the structure and function of an activated-sludge

microbial community against a 3-chloroaniline shock load. *Appl. Environ. Microbiol.* **69**, 1511–1520 (2003).
67. Douny, C. et al. Development of an analytical method to detect short-chain fatty acids by SPME-GC-MS in samples coming from an in vitro gastrointestinal model. *J. Chromatogr., Anal. Technol. Biomed. Life Sci.* **1124**, 188–196 (2019).
68. R Core Team, *R: A language and environment for statistical computing*, Vienna, Austria: R Foundation for Statistical Computing (2020).
69. Stan Development Team, «*Stan Modeling Language Users Guide and Reference Manual, version 2.31,*» 2022. [Online]. Available: https://mc-stan.org/docs/stan-users-guide/index.html. Accessed on Oct 1, 2022.
70. McElreath, R. *rethinking: A package for fitting and manipulating Bayesian models* (2020).
71. Bürkner, P. *brms: Bayesian Regression Models using 'Stan'* (2022).
72. Pedersen, T. *ggraph: An Implementation of Grammar of Graphics for Graphs and Networks* (2021).
73. Oksanen, J. et al. *vegan: Community Ecology Package* (2019).

Acknowledgements

We want to thank Léa Siegwald for her valuable input on *Bifidobacterium* subspecies annotation, Regula Müller-Schüpbach, Thierry Bénet and Sean Austin for their help with the human milk oligosaccharide quantification, Jens Stolte and Leen Baert for the development of the strain-specific qPCR assay, Catherine Gnom-Bru and Stéphane Duboux for the critical reading of the manuscript, Norbert Sprenger for his help with defining the HMO mixes, and Sophia Zhang for her infant and toddler illustrations.

Author contributions

F.D.B. analyzed and compiled the data, K.Johnson and D.M. designed the experiments, F.D.B., K. James, and K. Johnson wrote the manuscript, G.C. developed the strain-specific qPCR assay, all authors reviewed the manuscript.

Competing interests

The authors declare the following competing interests: all authors are employees of Société des Produits Nestlé S.A.

Additional information

Supplementary information The online version contains supplementary material available at https://doi.org/10.1038/s42003-024-06628-1.

Correspondence and requests for materials should be addressed to Florac De Bruyn.

Peer review information *Communications Biology* thanks Francesca Turroni and the other, anonymous, reviewer(s) for their contribution to the peer review of this work. Primary Handling Editors: Sabina Leanti La Rosa and Tobias Goris.

Reprints and permissions information is available at http://www.nature.com/reprints

Publisher's note Springer Nature remains neutral with regard to jurisdictional claims in published maps and institutional affiliations.

Open Access This article is licensed under a Creative Commons Attribution-NonCommercial-NoDerivatives 4.0 International License, which permits any non-commercial use, sharing, distribution and reproduction in any medium or format, as long as you give appropriate credit to the original author(s) and the source, provide a link to the Creative Commons licence, and indicate if you modified the licensed material. You do not have permission under this licence to share adapted material derived from this article or parts of it. The images or other third party material in this article are included in the article's Creative Commons licence, unless indicated otherwise in a credit line to the material. If material is not included in the article's Creative Commons licence and your intended use is not permitted by statutory regulation or exceeds the permitted use, you will need to obtain permission directly from the copyright holder. To view a copy of this licence, visit http://creativecommons.org/licenses/by-nc-nd/4.0/.

© The Author(s) 2024